npj | vaccines

Article

Published in partnership with the Sealy Institute for Vaccine Sciences

https://doi.org/10.1038/s41541-025-01275-x

Cocktail vaccine induces immunoprotection and modulates the fecal microbiota in dogs against *Echinococcus granulosus* infection

Guoqing Shao[1], Xiaowei Zhu[1], Ruiqi Hua[1], Zhiwei Lu[1], Yanxin Chen[1], Aiguo Yang[2] & Guangyou Yang[1] ✉

Cystic echinococcosis (CE) is a global zoonotic parasitic disease that represents a significant public health challenge. Although vaccination is considered an ideal strategy for controlling CE, no effective vaccines are currently available for dogs. Herein, bioinformatic approaches were employed to identify vaccine candidates. The selected proteins, including *Echinococcus granulosus* enolase (*Eg*ENO), severin (*Eg*Sev), cyclophilin (*Eg*Cyc), fatty acid-binding protein 1 (*Eg*FABP1), calmodulin (*Eg*CaM), and serine protease inhibitor 1 (*Eg*Srp1), were expressed in *Escherichia coli*. These proteins were grouped into cocktail vaccines: r*Eg*ENO&r*Eg*Sev&r*Eg*Cyc and r*Eg*FABP1&r*Eg*CaM&r*Eg*Srp1, and were combined with the Quil-A adjuvant to evaluate vaccine efficacy in beagles. After two subcutaneous immunizations, the r*Eg*ENO&r*Eg*Sev&r*Eg*Cyc and r*Eg*FABP1&r*Eg*CaM&r*Eg*Srp1 vaccines reduced the parasite burden by 80.58% ($p < 0.01$) and 47.92% ($p < 0.01$), respectively. Additionally, *Ligilactobacillus*, *Fusobacterium*, and *Streptococcus* correlated significantly with immunoprotection. This study demonstrated bioinformatically screened antigens were effective vaccine candidates, and vaccine-microbiota interactions provided a potential strategy to improve vaccine efficacy.

Echinococcus granulosus sensu lato (*E. granulosus* s.l.), a cestode residing in the intestinal tract of canids, is the causative agent of cystic echinococcosis (CE), a globally prevalent zoonotic disease characterized by the establishment of its metacestodes in the organs of livestock (e.g., sheep, goats, cattle, yaks, pigs, horses, camels) and humans[1]. This disease poses significant threats to both public health and livestock economies, leading to considerable socioeconomic burdens[2]. Recognizing its impact, the World Health Organization (WHO) has included CE in its 2021–2030 strategic plan for control or elimination[3,4]. As definitive hosts, dogs serve as the primary source for CE infection, facilitating transmission to humans and animals primarily through the ingestion of food or water contaminated with feces containing *E. granulosus* eggs[5]. The current strategy to control *E. granulosus* infection in dogs relies on monthly praziquantel-based deworming programs[6]. However, this approach is hindered by significant challenges, including high resource demands and the emergence of anthelmintic resistance caused by prolonged drug use, ultimately undermining intervention efficacy[7,8].

With further advances in our understanding of dogs' mucosal immune responses following *E. granulosus* infection, the development of effective vaccines for dogs is increasingly regarded as a cornerstone strategy to mitigate CE transmission[9,10]. Compared with intermediate hosts such as sheep, cattle, and yak, the relatively smaller canine population makes dog vaccination a potentially more cost-effective strategy[11,12]. Current research on dog vaccination against *E. granulosus* primarily focuses on screening protective antigens. Recently, studies have demonstrated that dog vaccination provides protection by reducing the parasite burden and suppressing its developmental progression[10,13,14]. Candidate vaccines, such as those comprising EgM family proteins[15,16], tropomyosin/paramyosin[17], 3-hydroxyacyl-CoA dehydrogenase[18], and the EgTIM-EgANXB3 (triose-phosphate isomerase and annexin B3) cocktail vaccine[19], have exhibited variable protective efficacy. To date, no vaccines have been licensed for use in dogs. A key challenge to commercialization is the inter-individual variability in protection rates, which compromises herd immunity and reduces the efficacy of population-level control[13,14].

[1]Department of Parasitology, College of Veterinary Medicine, Sichuan Agricultural University, Chengdu, Sichuan, PR China. [2]Sichuan Center for Animal Disease Prevention and Control, Chengdu, Sichuan, PR China. ✉e-mail: guangyou1963@126.com

The inter-individual variability in vaccine-induced protective efficacy is modulated by multiple intrinsic and extrinsic factors, including host genetic background, innate immune status, and nutritional conditions[20]. Recent studies have revealed significant correlations between the gut microbiota composition and vaccine efficacy[21–23]. Specifically, a higher abundance of *Actinobacteria* is positively associated with robust vaccine responses, whereas *Bacteroidetes* is linked to reduced immunogenicity. The association between *Firmicutes* and *Proteobacteria* abundance and vaccine responsiveness appears to be taxon-specific[24–28]. Nevertheless, research exploring vaccine-induced microbiota modulation remains limited, particularly in the context of parenteral immunization[20]. Notably, helminth infections lead to substantial microbiota remodeling[29,30], suggesting a potential interplay between parasite-induced dysbiosis and vaccine-mediated microbiota regulation. Determining this interaction could provide new insights into the mechanisms underlying vaccine-induced immunoprotection[20,31]. A systematic investigation into the correlation between vaccine-induced protection and alterations in fecal microbiota composition would provide valuable insights to develop next-generation vaccine adjuvants and delivery strategies.

In this study, we utilized bioinformatics to identify *E. granulosus* vaccine candidate antigens, followed by vaccination trials to systematically assess their efficacy and investigate the correlations between immunoprotection efficacy and fecal microbiota dynamics. Our findings provide a theoretical basis for controlling echinococcosis and offer novel insights into optimizing vaccine design.

Results

Bioinformatics-assisted identification of vaccine antigens

Proteomic profiling of exosomes identified 1916 high-confidence proteins. To establish a complete excretory/secretory (ES) proteome of adult *E. granulosus*, we integrated prior ES proteomic datasets, resulting in a catalog of 1940 proteins (Supplementary Table 1).

Through the multi-step antigen discovery pipeline, we identified 13 potential vaccine candidates: (1) Transcriptomic profiling of developmental stages revealed 439 genes that were significantly upregulated during parasite maturation (Supplementary Fig. 1a–c). (2) Comparative proteomic analysis via the Venn diagram intersection of protein datasets (Supplementary Table 1) identified 92 shared antigen candidates (Supplementary Fig. 2 and Supplementary Table 2). (3) Functional annotation based on literature mining further refined the selection to 15 well-characterized proteins. In silico antigenicity prediction using ANTIGENpro (cutoff ≥0.5) further identified 13 antigenic candidates (Table 1). Among them, triosephosphate isomerase (TIM), annexin B3 (ANXB3), and fatty acid-binding protein 2 (FABP2) have been validated as vaccine candidates with protective efficacy by our previous study[19]. Consequently, six proteins (r*Eg*ENO, r*Eg*Sev, r*Eg*Cyc, r*Eg*FABP1, r*Eg*CaM, r*Eg*Srp1) were prioritized for further vaccine development.

Recombinant protein expression

Six *E. granulosus* genes were successfully cloned and expressed. PCR amplification using cDNA templates derived from PSCs and strobilated worms yielded distinct bands corresponding to *Eg*ENO (1302 bp), *Eg*Sev (1101 bp), *Eg*Cyc (489 bp), *Eg*FABP1 (402 bp), *Eg*CaM (450 bp), and *Eg*Srp1 (1104 bp) (Supplementary Fig. 3a). Six recombinant proteins (r*Eg*ENO, r*Eg*Sev, r*Eg*Cyc, r*Eg*FABP1, r*Eg*CaM, and r*Eg*Srp1) were confirmed by the SDS-PAGE analysis. The molecular weights of the recombinant proteins, including the pET-32a (+) vector-derived tag, were consistent with their theoretically approximate values: r*Eg*ENO (65.7 kDa), r*Eg*Sev (58.4 kDa), r*Eg*Cyc (35.9 kDa), r*Eg*FABP1 (32.7 kDa), r*Eg*CaM (34.5 kDa), and r*Eg*Srp1 (58.5 kDa) (Supplementary Fig. 3b, c).

Vaccine-induced protection against *E. granulosus* in dogs

At 28 days post-challenge, necropsy was performed, which demonstrated varying levels of protection efficacy among the groups (Fig. 1 and Supplementary Table 3). In the control group, the worm burden in each dog reached 100,451 ± 10,340, with a mean worm length of 1.199 ± 0.014 mm and width of 0.199 ± 0.003 mm. The r*Eg*FABP1&r*Eg*CaM&r*Eg*Srp1 vaccine group exhibited a 47.92% reduction in worm burden compared with that of the control ($p < 0.01$), with 52,313 ± 8754 worms. Worm length showed a marked reduction by 15.51% ($p < 0.05$), whereas width remained comparable (Fig. 2 and Supplementary Table 4). Notably, the r*Eg*ENO&r*Eg*Sev&r*Eg*Cyc vaccine demonstrated superior efficacy, achieving an 80.58% reduction in worm burden ($p < 0.01$), with 19,511 ± 6621 worms. Additionally, worms exhibited 0.86 fewer proglottids, and 24.85% ($p < 0.01$) and 22.11% ($p < 0.01$) reductions in body length and width, respectively (Fig. 2 and Supplementary Table 4).

Histopathological evaluation

Histopathological analysis indicated some degree of vaccine-associated protection against intestinal damage caused by *E. granulosus* infection (Fig. 3a–c). Gross examination of control dogs showed diffuse mucosal edema and hemorrhagic exudates, whereas vaccinated groups generally exhibited better-preserved mucosal integrity. H&E staining demonstrated notable villus architectural disruption in control dogs, including immune cell infiltration at parasite attachment sites (Fig. 3a). Vaccinated dogs maintained well-preserved villus morphology, exhibiting fewer parasite adhesion sites (Fig. 3b, c). PAS staining showed strong mucin production across all groups. Notably, goblet cell density was elevated in the vaccinated dogs, consistent with parasite-driven mucus hypersecretion.

Serum IgG and cytokine dynamics

Serum IgG profiling (Fig. 4a–f) revealed distinct antibody kinetics among the vaccine groups. The r*Eg*FABP1&r*Eg*CaM&r*Eg*Srp1 group achieved high IgG titers at D21, but the levels had declined by D49, with greater inter-individual variation. Additionally, the r*Eg*ENO&r*Eg*Sev&r*Eg*Cyc group exhibited a robust IgG response, peaking at D21 and persisting at significantly higher levels than the control group ($p < 0.05$) until D49. Serum IgG longevity in dogs vaccinated with the r*Eg*ENO&r*Eg*Sev&r*Eg*Cyc vaccine suggested that antibody responses could be maintained for at least 6 months, potentially contributing to sustained immunoprotection (Fig. 4g–i).

Cytokine profiling (Fig. 4k) revealed a mixed Th1/Th2 response in the r*Eg*FABP1&r*Eg*CaM&r*Eg*Srp1 group at D21 after the second immunization, characterized by concurrent IL-2, IL-4, and IFN-γ upregulation ($p < 0.05$). Following parasite challenge (Day 35), levels of IL-2, IL-4, and IFN-γ significantly decreased ($p < 0.05$), suggesting a suppression of host immune responses. Interestingly, the r*Eg*ENO&r*Eg*Sev&r*Eg*Cyc group displayed a unique immune response (Fig. 4l). While cytokine levels remained unchanged at D21, a pronounced Th2-skewed immunity occurred at D35 post-challenge, characterized by significant IL-4 and IL-10 upregulation ($p < 0.05$) and IL-2 suppression below the detection limit. Furthermore, IFN-γ levels rose significantly at D35 ($p < 0.05$), indicating IFN-γ pathway activation.

Alpha diversity and beta diversity analysis of the fecal microbiota composition

To investigate the interplay between the fecal microbiota and vaccine-induced immune responses, we performed 16S rRNA gene sequencing to profile fecal microbiota composition. Comparative analysis of the three experimental groups (Fig. 1) demonstrated dynamic shifts in microbial diversity at both the phylum and genus levels throughout the vaccination process and *E. granulosus* infection (Supplementary Fig. 4).

Analysis of longitudinal α-diversity (Fig. 5a–f) revealed distinct microbial community shifts in dogs in the r*Eg*ENO&r*Eg*Sev&r*Eg*Cyc vaccine group (Fig. 5e, f). Shannon and Chao1 indices exhibited significant increases at 7 days post-secondary immunization (D21, $p < 0.05$) relative to baseline (D0), indicating a vaccine-mediated expansion of microbial diversity. The sustained elevation of the Shannon index at 14 days post-challenge (D35, $p < 0.05$) suggested that microbiota remodeling might contribute to enhanced host immune defense. In contrast, the dogs in the

https://doi.org/10.1038/s41541-025-01275-x

Table 1 | Summary of candidate proteins for vaccination against *Echinococcus granulosus* in dogs

Number	Protein	Accession number (UniProtKB)	Antigenicity	Identity rate with *Echinococcus multilocularis*	Transcriptome Adult PSC		AW ES products	PSC ES products	Cross-species interaction proteins	Associated publications (PubMed ID)
					log2(Fold_change)	*p* value				
1	Heat shock 70 kDa protein	A0A068X4W2	0.96	–	–	–	Y	N	Y	23485966;28576342;12911519
2	Calreticulin	W6U953	0.95	96.40%	3.612905779	0.007191408	Y	N	N	17936905; 24013640;17936905
3	*Cyclophilin*[a]	P14088	0.92	99.40%	–	–	Y	N	Y	12458833; 2677720;12458833;11982600;23012952
4	Fatty acid-binding protein 2	U6JIF2	0.91	96.60%	1.9232459	0.000734653	Y	N	N	24013640; 23485966;32130486;37871121
5	*Calmodulin*[a]	U6JA54	0.90	97.50%	0.92569322	0.007693969	Y	N	N	24013640; 23485966;29202858;33845889;30846822;25818323
6	Superoxide dismutase	W6V988	0.86	98.70%	–	–	Y	N	Y	24013640;7668094;17432620
7	*Severin*[a]	U6IX85	0.82	98.60%	–	–	Y	Y	Y	24013640; 23485966;37060967
8	14-3-3 protein	Q56J98	0.76	98.40%	1.141967735	5.21742E-16	Y	Y	Y	24013640; 23485966;22840587
9	Triosephosphate isomerase	U6JN02	0.67	98.80%	–	–	Y	N	Y	24013640; 23485966;30027383;27283960;37871121
10	*Fatty acid binding protein*[a]	A0A068WTS7	0.60	–	4.136467735	1.55061E-21	Y	N	N	23485966;26873273;32130486;11731339;12818189;23166848;9169781;-9777493;15007640
11	*Serine protease inhibitor*[a]	U6FVI6	0.59	92.90%	0.825314112	0.003911208	Y	N	N	23485966;19759914;28192542
12	*Enolase*[a]	D0VLV3	0.53	98.60%	–	–	Y	N	Y	20127115; 23485966;31508329;22750316;20127115;23373261
13	Annexin	A0A068WJF9	0.50	98.80%	–	–	Y	N	Y	23485966;37803469;33557917;37871121
14	Citrate synthase	U6J0K5	0.43	98.70%	–	–	Y	N	Y	24013640; 23485966;31049696
15	Malate dehydrogenase	A0A068WYB8	0.43	99.70%	–	–	Y	N	Y	23485966;15383291;8352009;8366891

Y yes, include, *N* no, not include, *AW E. granulosus* adult worm, *PSC E. granulosus* protoscolex, *ES products* excretory/secretory products.

[a]The protein names in *italics* are candidate proteins for vaccination in this study.

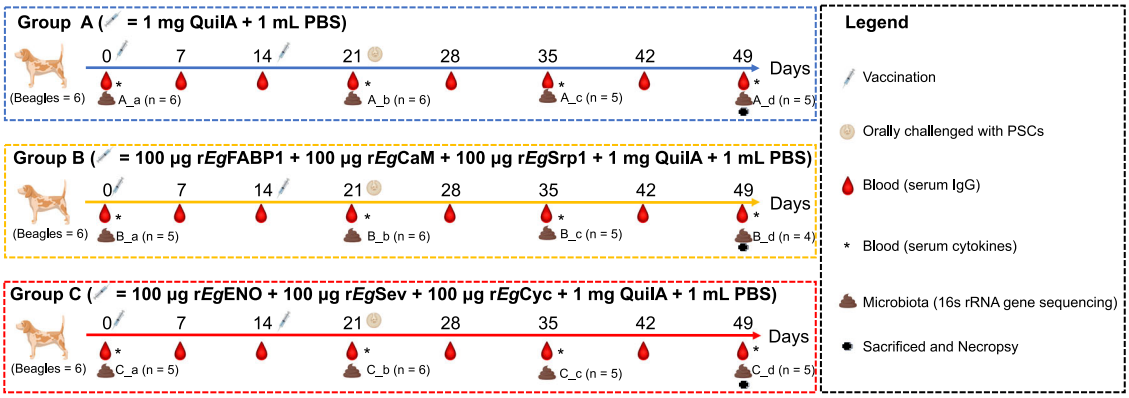

Fig. 1 | Overview of the experimental framework, including vaccination schedule, parasite challenge, and sampling timeline. Schematic summary of the study design, including the vaccination regimen and sample collection across three experimental groups. The timeline illustrates the major experimental procedures, including vaccination, parasite challenge, and designated sampling points (marked above the timeline). Stool and blood samples were obtained at specified time points (indicated by specific labels) for 16S rRNA sequencing and assessment of serum IgG levels and cytokine dynamics. Sample labels: A_a: Group A, time point Day0; A_b: Group A, Day21; A_c: Group A, Day35; A_d: Group A, Day49. B_a: Group B, Day0; B_b: Group B, Day21; B_c: Group B, Day35; B_d: Group B, Day49. C_a: Group C, Day0; C_b: Group C, Day21; C_c: Group C, Day35; C_d: Group C, Day49.

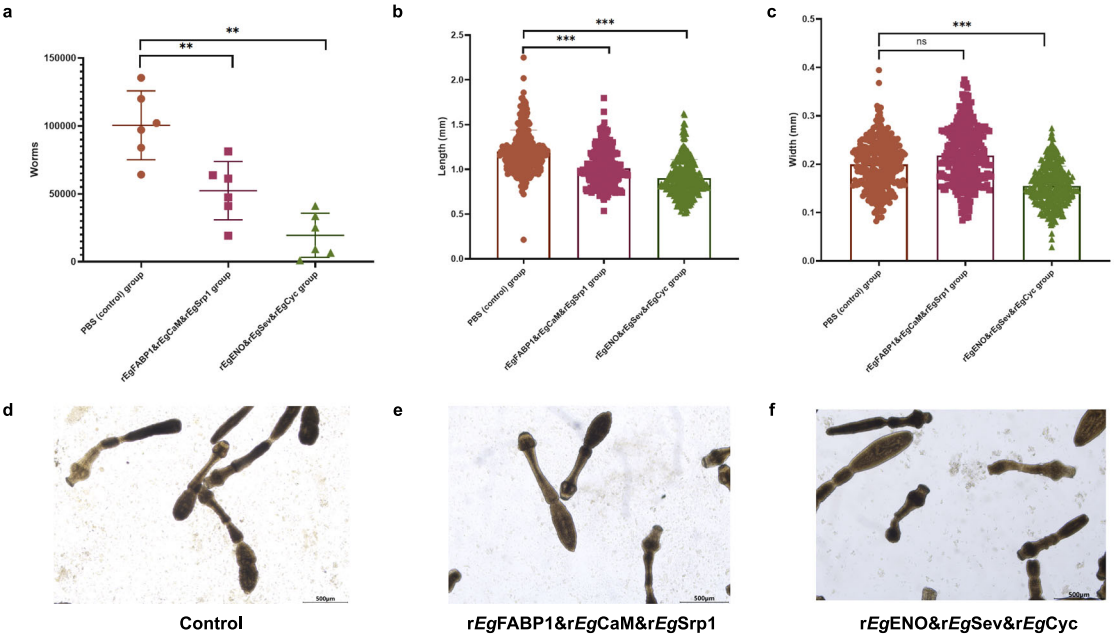

Fig. 2 | Assessment of vaccine-induced protection against *E. granulosus* infection in dogs. Quantitative evaluation of parasite burden and morphology, including **a** worm burden reduction, **b** worm length, and **c** worm width at 49 days post-infection across the experimental groups. Representative micrographs of 28-day worms from **d** the control group, **e** the r*Eg*FABP1&r*Eg*CaM&r*Eg*Srp1 group, and **f** the r*Eg*ENO&r*Eg*Sev&r*Eg*Cyc group. Scale bar: 500 μm. Data are presented as mean ± SEM; $*p < 0.05$, $**p < 0.01$, $***p < 0.001$.

r*Eg*FABP1&r*Eg*CaM&r*Eg*Srp1 group exhibited microbiota dysregulation (Fig. 5c, d), with a transient increase in the Shannon index at D21, followed by a sustained decline post parasite challenge, leading to a significant decrease at D49 ($p < 0.05$). Meanwhile, the Chao1 indices remained statistically unchanged. To assess vaccine-specific effects on α-diversity dynamics, control group analyses were conducted. The control group exhibited a progressive decline in both Shannon and Chao1 indices throughout the study, with a significant reduction at D35 post-challenge ($p < 0.05$, Fig. 5a, b), confirming the parasite's ability to suppress microbiota diversity. The divergence between vaccinated and control groups suggested that vaccine antigens might counteract parasite-driven microbial adaptations by modulating the fecal microbiota composition.

Analysis of β-diversity (Fig. 5g–i) demonstrated distinct vaccine-mediated clustering of r*Eg*ENO&r*Eg*Sev&r*Eg*Cyc samples along the PC1 and PC2 coordinates (ANOSIM: $R = 0.7636$, $p = 0.001$). Principal coordinate analysis (PCoA) based on Bray–Curtis distances revealed that PC1 (32.36%) and PC2 (19.39%) explained 51.75% of the total variance, suggesting dynamic, vaccine-induced shifts in the fecal microbiota composition. In contrast, the control group exhibited substantial post-parasite challenge displacement along PC1 (27.32%) and PC2 (16.64%) (ANOSIM: $R = 0.5876$, $p = 0.001$), forming a distinct clustering pattern relative to the vaccinated groups.

Variability of the fecal microbiota in vaccinated or *E. granulosus*-infected dogs

To investigate the impact of *E. granulosus* infection and vaccination on fecal microbiota regulation, longitudinal dynamic analysis was performed, revealing intervention-specific taxonomic alterations. By analyzing the top

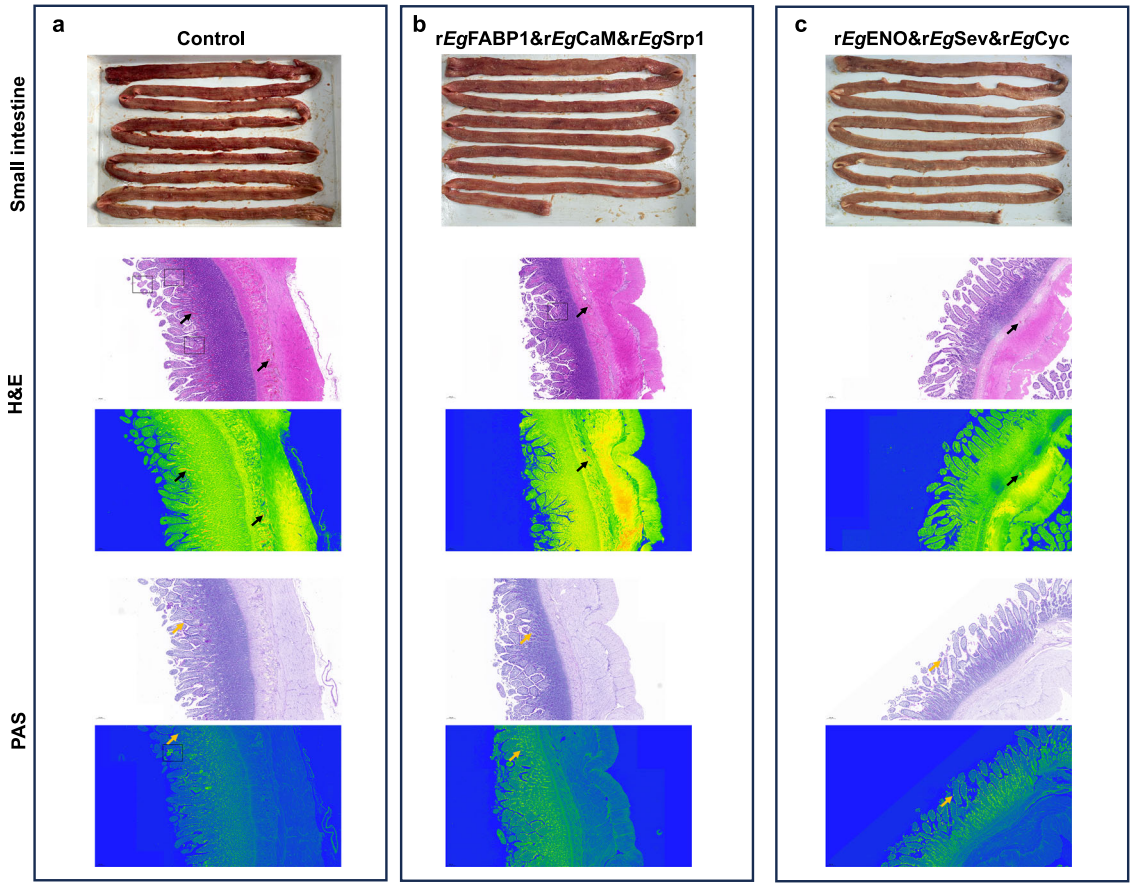

Fig. 3 | Analysis of histopathological changes in the small intestine on day 49. Small intestines collected from dogs in the control (**a**) and vaccinated groups (**b**, **c**) (r*Eg*FABP1&r*Eg*CaM&r*Eg*Srp1 and r*Eg*ENO&r*Eg*Sev&r*Eg*Cyc) at 4 weeks post-PSC challenge and processed for H&E and PAS staining. Parasite attachment sites, hemorrhagic exudates, and goblet cells were indicated by black frames, black arrows, and yellow arrows, respectively. Scale bar: 200 μm.

10 core bacterial genera (Figs. 6a, 7a), combined with LEfSe analysis (LDA > 3.5, FDR-corrected $p < 0.05$ via Kruskal–Wallis test; Figs. 6b, 7b), identified three key taxa—*Ligilactobacillus* (phylum Firmicutes), *Fusobacterium* (phylum Fusobacteria), and *Streptococcus* (phylum Firmicutes)—exhibiting distinct responses to vaccination and *E. granulosus* infection.

In the control group, following *E. granulosus* colonization (D35), the relative abundance of *Ligilactobacillus* increased by 33.98% ($p = 0.008$) and that of *Streptococcus* increased by 7.87% ($p = 0.014$), whereas *Fusobacterium* exhibited a 9.46% decline ($p = 0.014$) (Fig. 6d). Conversely, the r*Eg*ENO&r*Eg*Sev&r*Eg*Cyc vaccine group exhibited an inverse regulatory trend (Fig. 7a–d), with *Ligilactobacillus* and *Streptococcus* abundances decreasing by 13.03% ($p = 0.008$) and 27.28% ($p = 0.008$), respectively, while *Fusobacterium* levels increased by 5.76% ($p = 0.007$) (Fig. 7d).

LEfSe analysis further confirmed *Ligilactobacillus* (LDA = 5.23/4.79), *Fusobacterium* (LDA = 4.78/4.43), and *Streptococcus* (LDA = 4.66/5.15) as key discriminative taxa across both experimental groups (Wilcoxon test, FDR-adjusted $p < 0.05$) (Figs. 6b and 7b). These findings suggested that vaccination might counteract *E. granulosus*-induced microbiota dysbiosis by modulating the relative abundances of key bacterial taxa.

Links between vaccine-induced immunity and fecal microbiota alterations

Building on previous evidence linking host immunity with the gut microbiota[32], we employed a multidimensional integrative approach to determine the relationship between vaccine-induced immune responses and microbiota alterations. Environmental factor analysis revealed significant dynamic covariation between the relative abundances of *Ligilactobacillus*, *Fusobacterium*, and *Streptococcus* and the host Th1/Th2 cytokine profiles (Fig. 8a).

Mantel tests and redundancy analysis (RDA) identified IFN-γ as the principal factor of microbiota restructuring following vaccination (Mantel's $r = 0.79$, $p = 0.01$). IFN-γ exhibited a strong positive correlation with IL-4 and IL-10, while showing a negative association with IL-2 (Fig. 8b). These findings suggested that the Th1/Th2 equilibrium plays a pivotal role in orchestrating temporal microbial shifts. Notably, RDA constrained 24.42% of microbiota variance (RDA1: 17.60%, RDA2: 6.82%; $p < 0.001$) (Fig. 8c), with IFN-γ ($r = 0.79$, $p = 0.01$, Mantel test) accounting for the highest proportion of constrained variation. These findings highlighted vaccine-induced host immune shifts as a key determinant of microbiota remodeling.

Discussion

Cystic echinococcosis (CE), caused by *E. granulosus*, remains a global public health challenge, imposing significant burdens on both human health and livestock productivity[3,33]. Given the chronic and complex nature of CE, control strategies should prioritize simple, cost-effective, and efficient approaches[6,7,14]. Vaccination, widely regarded as the most cost-effective approach of infectious disease control[34], holds great promise for CE prevention. Moreover, mathematical models of *E. granulosus* transmission dynamics have further demonstrated that vaccinating dogs can reduce infection pressure on intermediate hosts; if herd immunity reaches 75%, parasite elimination may be achievable[35]. However, the lack of effective commercial vaccines for dogs—the primary definitive hosts and reservoirs of *E. granulosus*—remains a critical barrier in CE eradication[10,13,14].

The complex life cycle of *E. granulosus*, involving multiple host transitions[5], facilitates its sophisticated immune evasion strategies[36–38]. This complexity poses a significant challenge in identifying antigens with high protective efficacy, constituting a major bottleneck in vaccine development. Traditional antigen screening approaches, which rely on animal infection

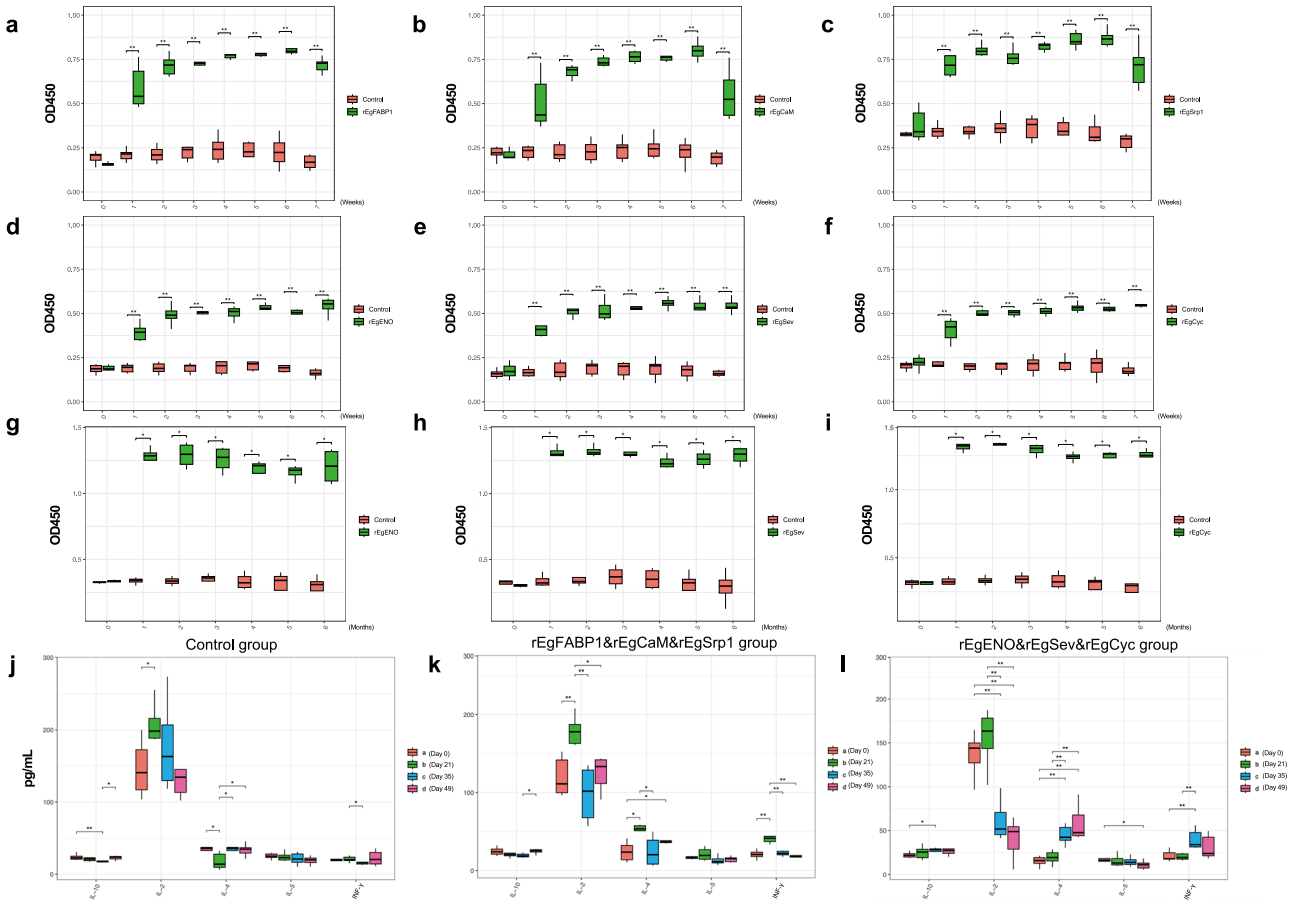

Fig. 4 | Serum-specific IgG and cytokine responses in dogs following immunization and challenge. Serum-specific IgG levels against r*Eg*FABP1 (**a**), r*Eg*CaM (**b**), r*Eg*Srp1 (**c**), r*Eg*ENO (**d**), r*Eg*Sev (**e**), and r*Eg*Cyc (**f**) in the experimental groups. Serum IgG longevity. Serum-specific IgG levels against r*Eg*ENO (**g**), r*Eg*Sev (**h**), r*Eg*Cyc (**i**) over 6 months. **j**–**l** Cytokine response patterns. **j** In the control group, IL-2 levels increased significantly at day 21, whereas IL-4 levels decreased, indicating a Th1-skewed response. **k** In the r*Eg*FABP1&r*Eg*CaM&r*Eg*Srp1 group, IL-2, IL-4, and IFN-γ levels increased significantly at day 21. **l** In dogs vaccinated with r*Eg*ENO, r*Eg*Sev, and r*Eg*Cyc, no notable cytokine fluctuations were observed at day 21. Post PSCs challenge, the IL-2 levels decreased, whereas the IL-4 and IL-10 levels increased, favoring a Th2-biased response. $^{*}p < 0.05$, $^{**}p < 0.01$, $^{***}p < 0.001$.

models, are hindered by lengthy experimental timelines, high costs, and biosafety concerns, severely restricting progress in vaccine research[9,14]. The integration of multi-omics data with bioinformatics provides an innovative strategy to identify novel vaccine antigens[39]. Based on the developmental biology of *E. granulosus*, key biological processes, such as PSC growth, adaptation to the intestinal environment, and immune evasion, are mediated by specific functional proteins[40]. These proteins, critical for parasite survival and host-parasite interactions, represent promising candidate targets for dog vaccines.

This study firstly established a comprehensive proteomic database of EVs from 28-day *E. granulosus*, integrating three functional protein subsets based on *E. granulosus* biological processes. Bioinformatic screening identified thirteen annotated proteins, including three previously validated vaccine candidates[19]. Based on this selection framework, six of the remaining ten proteins were prioritized for vaccine efficacy assessment. These proteins were tegument-localized or *E. granulosus* secreted proteins likely to interact directly with the host intestinal mucosa, thereby triggering antigen-specific immune responses[41,42]. Notably, *Eg*ENO functions not only as a glycolytic enzyme essential for parasite energy metabolism, but also as a major exosome component in adult worms, playing a role in host immune modulation[43]. Similarly, the tegument-localized *Eg*Sev protein is presumed to facilitate parasite motility via mechanisms similar to those of *Eg*A31[44,45]. Bioinformatic profiling of *Eg*Cyc identified highly immunogenic epitopes, reinforcing its potential as a vaccine candidate[46]. *Eg*FABP1, a lipid trafficking protein crucial for parasite survival[16], mediates host-derived lipid acquisition essential for growth and development[40], while exhibiting strong immunogenic properties for vaccination[47]. Functional analyses of *Eg*CaM[48,49] and *Eg*Srp1[50,51] further delineated their roles in parasite maturation and adaptation to the gut microenvironment. Collectively, these findings confirm the reliability of our bioinformatics-driven vaccine antigen discovery framework. Additionally, antigen delivery strategies significantly influence vaccine efficacy. The antigenic complexity of multicellular helminths such as *E. granulosus* means that single-antigen vaccines might be insufficient to provide immunoprotection because of epitope diversity[52]. Cocktail vaccines provide a viable approach to enhance protective efficacy and durability, representing a promising direction in antiparasitic vaccine development[53,54]. Our cocktail vaccines were designed to align with this approach.

Building upon these foundational studies, our cocktail vaccine (r*Eg*ENO&r*Eg*Sev&r*Eg*Cyc) achieved an 80.58% reduction in the worm burden following a two-dose immunization regimen, representing an approximately 10% improvement over existing two-dose vaccines[19]. Comparative analysis highlighted three key advantages: (1) The two-dose subcutaneous regimen confers enhanced protection against high-dose PSC challenge, while maintaining operational feasibility; (2) sustained antibody levels for 6 months post-immunization support a biannual vaccination strategy to prevent parasite establishment; (3) high sequence homology (>98%) with *Echinococcus multilocularis* homologous antigens (Table 1) suggests potential cross-protection against both cestode species[10]. Dogs also serve as

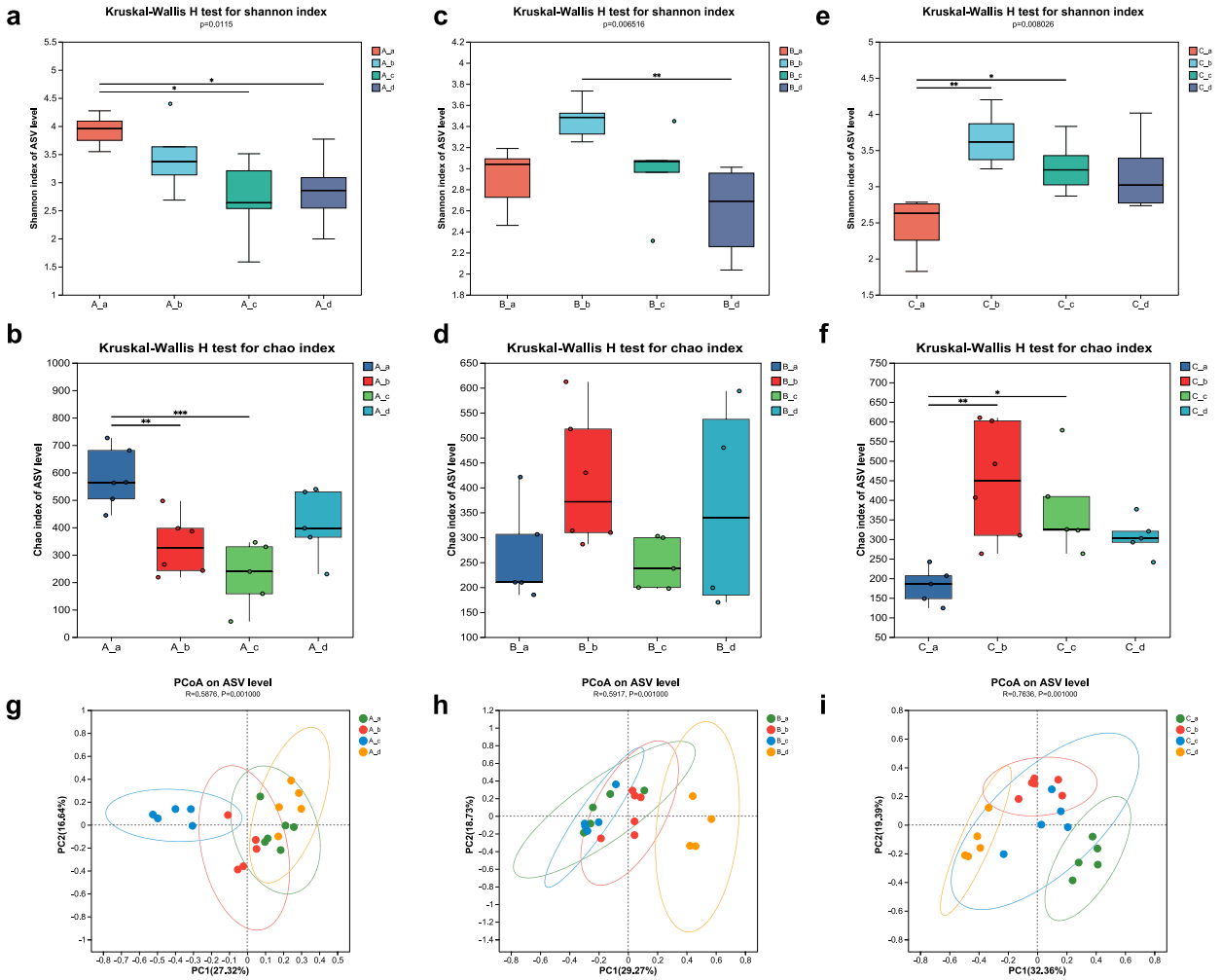

Fig. 5 | Changes in fecal microbiota diversity and composition in dogs following immunization and PSC challenge. a–f Temporal α-diversity analysis (Shannon and Chao1 indices). In the control group, both indices exhibited a continuous decline, with a significant reduction observed at day 35 ($p < 0.05$) (**a**, **b**). In the r*Eg*FABP1&r*Eg*CaM&r*Eg*Srp1 group, the Shannon index showed a transient increase at day 21, followed by a progressive decline that became significant at day 49 ($p < 0.05$), whereas the Chao1 index remained unchanged (**c**, **d**). In the r*Eg*ENO&r*Eg*Sev&r*Eg*Cyc group, both the Shannon and Chao1 indices increased significantly at day 21 and day 35 ($p < 0.05$) (**e**, **f**). **g–i** β-diversity analysis based on Bray–Curtis distance. Principal coordinate analysis (PCoA) revealed distinct clustering of fecal microbiota from the control (**g**), r*Eg*FABP1&r*Eg*CaM&r*Eg*Srp1 (**h**), and r*Eg*ENO&r*Eg*Sev&r*Eg*Cyc (**i**) groups. Sample labels: A_a: Group A, Day0; A_b: Group A, Day21; A_c: Group A, Day35; A_d: Group A, Day49. B_a: Group B, Day0; B_b: Group B, Day21; B_c: Group B, Day35; B_d: Group B, Day49. C_a: Group C, Day0; C_b: Group C, Day21; C_c: Group C, Day35; C_d: Group C, Day49.

definitive hosts of *E. multilocularis*, and in many CE-endemic areas, alveolar echinococcosis coexists as a major concern in Central Asia and western China, where *E. multilocularis* and *E. granulosus* exhibit high endemicity[1,10,14]. Given the absence of licensed vaccines against *E. multilocularis*[55], the cross-protective potential of the vaccine developed in the present study holds substantial socioeconomic and public health significance for the simultaneous control of CE and alveolar echinococcosis within endemic regions.

Although existing candidate vaccines against *E. granulosus* induce variable protective responses in dogs, substantial inter-individual differences in vaccine efficacy have been reported[14]. A substantial proportion of low responders might hinder herd immunity development, thereby reducing overall disease control effectiveness[56]. Thus, unraveling the complex host-parasite interactions and immune protection mechanisms of *E. granulosus* is essential to optimize vaccination strategies. Recent studies highlighted the gut microbiota composition as a pivotal determinant of vaccine efficacy[56,57]. However, the relationships between *E. granulosus* infection, microbiome dynamics, and vaccine efficacy have yet to be explored in canine models.

This study provides the first comprehensive characterization of the interactions between *E. granulosus* infection, fecal microbiota alterations, and vaccine-mediated immunity, offering novel insights into vaccine response variability. Experimental validation confirmed that *E. granulosus* infection drives distinct fecal microbiota remodeling in dogs. Unlike typical helminth infections that promote α-diversity[29], *E. granulosus* infection significantly decreased the Shannon index ($p < 0.05$) while increasing *Ligilactobacillus* and *Streptococcus* abundance and suppressing *Fusobacterium*. These microbial alterations might enhance parasite survival through three mechanisms: (1) *Ligilactobacillus*-derived lactate might disrupt mucosal immune surveillance by modulating dendritic cell-T cell interactions, thereby facilitating immune evasion[58]; (2) *Streptococcus* enrichment might sustain parasite-favorable microenvironments by modulating metabolic reprogramming[59]. Notably, the depletion of *Fusobacterium* mirrors patterns observed in enterobiasis[60], suggesting the presence of a conserved helminth-driven immunoregulatory mechanism. Collectively, these findings suggest that *E. granulosus* strategically manipulates its ecological niche through targeted microbiota modulation.

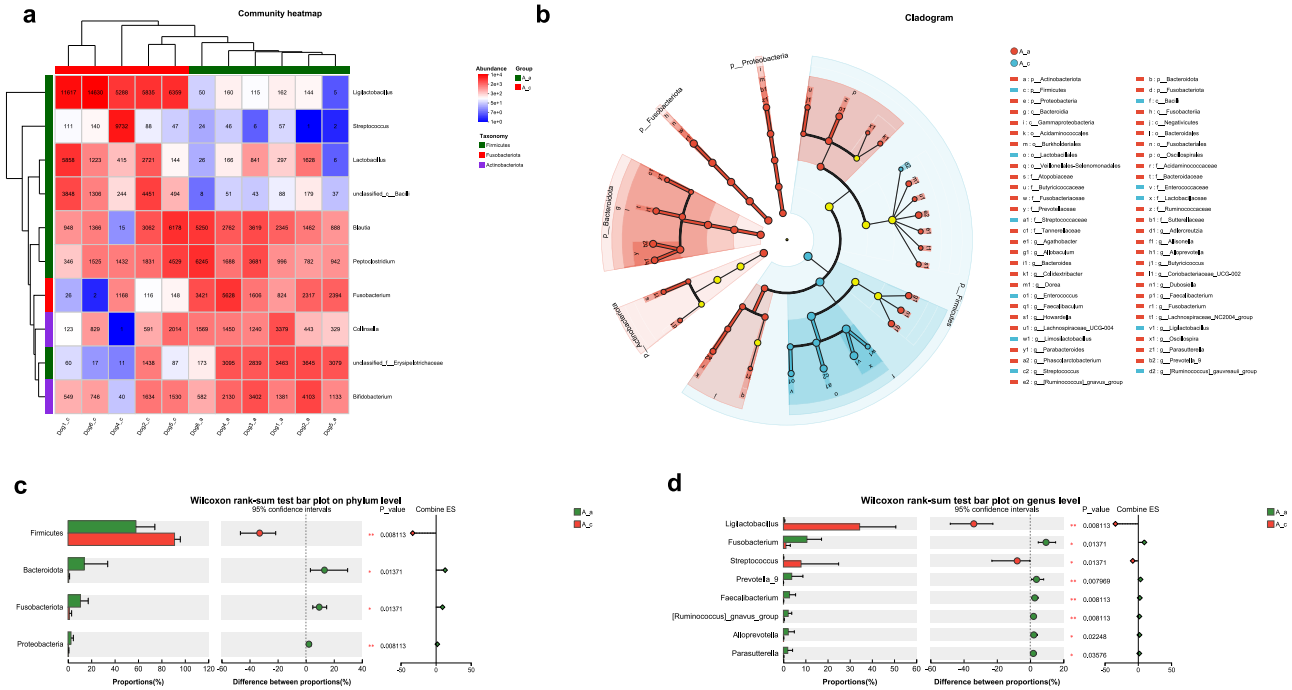

Fig. 6 | Dynamics of fecal microbiota composition following *E. granulosus* infection. a Heatmap illustrating relative abundance changes in the top 10 bacterial genera. **b** LEfSe analysis (LDA score >3.5, $p < 0.05$) identifying key discriminative taxa. **c** Fecal microbiota composition changes at the phylum level. **d** Genus-specific relative abundance shifts. Sample labels: A_a: Group A, Day0; A_c: Group A, Day35.

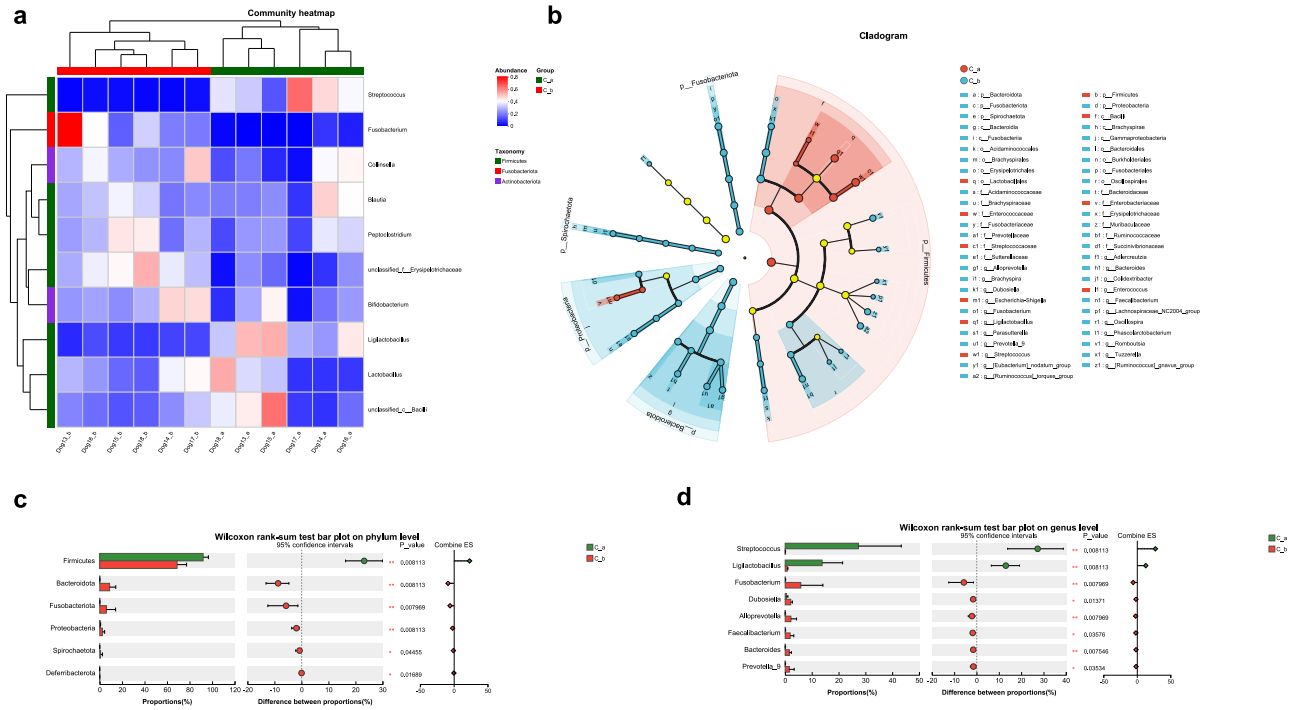

Fig. 7 | Fecal microbiota alterations following immunization with the r*Eg*ENO&r*Eg*Sev&r*Eg*Cyc vaccine. a Heatmap illustrating relative abundance changes in the top 10 bacterial genera before and after vaccination. **b** LEfSe analysis (LDA score >3.5, $p < 0.05$) identifying key discriminatory taxa. **c** Phylum-level compositional alterations. **d** Genus-specific relative abundance variations post-vaccination. Sample labels: C_a: Group C, Day0; C_b: Group C, Day21.

The r*Eg*ENO&r*Eg*Sev&r*Eg*Cyc vaccine, which exhibited the highest efficacy in reducing *E. granulosus* burden in this study, comprises ES antigens from adult worms that are potentially involved in host-parasite interactions[42,61]. To investigate the microbiota-immunity interplay underpinning anthelmintic protection, comparative analyses between the high-efficacy vaccine groups and controls revealed inverse abundance patterns of *Ligilactobacillus*, *Fusobacterium*, and *Streptococcus*. Vaccine-induced microbiota remodeling was observed to influence *E. granulosus* colonization, thereby contributing mechanistically to protective immunity. Notably, longitudinal variations in

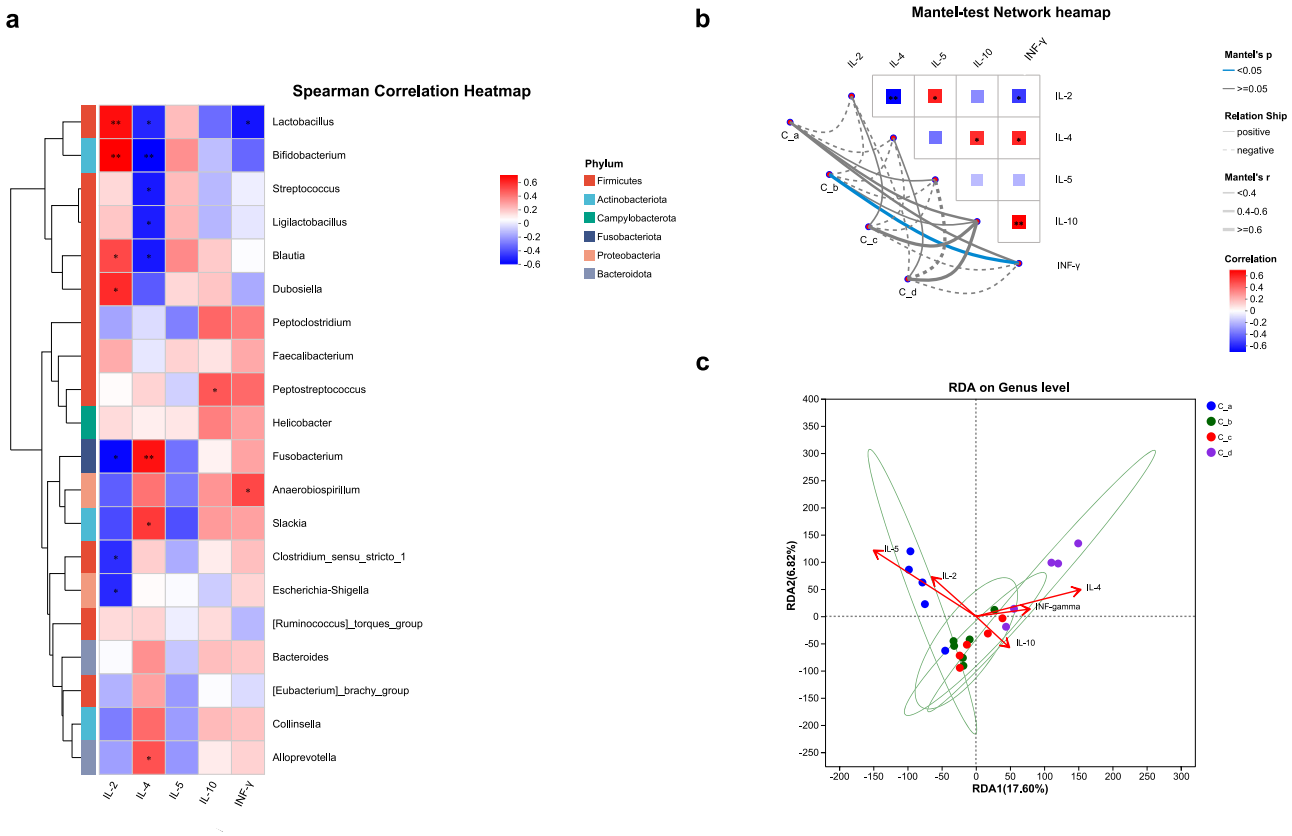

Fig. 8 | Interaction networks between cytokines and fecal microbiota under the r*Eg*ENO&r*Eg*Sev&r*Eg*Cyc vaccine-induced immunity. a Heatmap of Pearson's correlation analysis between key bacterial genera and cytokine levels. **b** Mantel test and RDA of cytokine-microbiota interactions. **c** RDA ordination plot illustrating the contributions of cytokines to microbiota variation. The first two constrained axes explained 24.42% of total microbiota variability (RDA1: 17.6%, RDA2: 6.82%, $p < 0.001$). Sample labels: C_a: Group C, Day0; C_b: Group C, Day21; C_c: Group C, Day35; C_d: Group C, Day49.

Ligilactobacillus, *Fusobacterium*, and *Streptococcus* abundances correlated positively with IL-4 concentrations in vaccinated dogs, supporting a Th2-skewed immune response that promoted parasite clearance and mitigated intestinal pathology[62]. Simultaneously, IFN-γ fluctuations exhibited microbiota-dependent associations, suggesting that vaccine-induced IFN-γ production might sustain long-term protection through interactions with microbial communities[63]. These findings provide novel insights to optimize vaccine design to enhance efficacy. However, this study is limited in its ability to identify specific bacterial species and to elucidate the mechanisms underlying microbiota-mediated modulation of host immunity. Future studies employing metagenomic sequencing and mechanistic approaches are warranted to further clarify the roles of key microbial taxa in shaping vaccine-induced protection.

Methods

Animals and parasites

A total of 22 6-month-old beagles (11 males and 11 females) were obtained from the Beagle Breeding Center at the Sichuan Institute of Musk Deer Breeding (Sichuan, China). Eighteen dogs were used for vaccine efficacy assessment and fecal microbiome dynamics assessment. Four were used to assess serum IgG longevity in vaccinated dogs. All dogs were housed under specific-pathogen-free conditions in a controlled quarantine facility and fed a standardized diet of commercial dog food with free access to tap water.

Hydatid cysts were harvested from the livers of sheep naturally infected with CE and slaughtered at an abattoir in Sichuan Province, China. Protoscoleces (PSCs) were isolated from these cysts following the methods described in our previous study[19]. The viability of the PSCs exceeded 95% were used for vaccine trials. Species identification was performed via PCR amplification and sequencing, confirming the *E. granulosus* sensu stricto G1 genotype[64].

Bioinformatics-assisted screening of vaccine candidates

Based on our previously acquired mass spectrometry proteomics dataset of adult *E. granulosus* exosomes, raw spectral data were analyzed using Mascot v2.3.02[65] against the UniProt database under rigorous quality control criteria (false discovery rate [FDR] ≤1%). This study employed a multi-step vaccine antigen screening pipeline by integrating our 28-day *E. granulosus* worm-derived exosome proteomic profile with publicly available *E. granulosus* proteomic and transcriptomic datasets[40–42,61,66,67]: (1) Comparative transcriptomics identified genes functionally upregulated in adult worms relative to PSCs (log2fold-change >2, $p < 0.05$) through volcano plot analysis; (2) gene selection was refined using threshold-optimized multi-group volcano plots and GO clustering, focusing on host-parasite interaction and immune evasion genes; (3) Four protein sets were constructed based on the multi-omics data, with the selection rationale detailed in Supplementary Table 1. Notably, cross-species interaction proteins were identified through Western blot analysis of the *E. granulosus* proteome using sera from infected dogs. Then, Venn diagram analysis was used to identify proteins shared among at least two sets, prioritizing those essential proteins for vaccine candidates. Antigenicity was predicted using ANTIGENpro (http://scratch.proteomics.ics.uci.edu/) with a cut-off value of ≥0.5, while cross-species protection potential was evaluated through BLAST (https://www.uniprot.org/blast) alignment against *Echinococcus multilocularis* orthologs.

Protein expression

The six recombinant *E. granulosus* proteins (r*Eg*ENO (enolase), r*Eg*Sev (severin), r*Eg*Cyc (cyclophilin), r*Eg*FABP1 (fatty acid-binding protein 1), r*Eg*CaM (calmodulin) and r*Eg*Srp1 (serine protease inhibitor 1) were expressed as follows. Primers with homologous arms were designed using Primer Premier 5.0 (Premier Biosoft, San Francisco, CA, USA) based on target sequences obtained from GenBank (Supplementary Table 5).

The target genes were amplified by PCR, and the amplicons were verified via 1% agarose gel electrophoresis before being inserted into the pET-32a (+) expression vector (Invitrogen, USA) using a Seamless Cloning Kit (Genesand Biotech, China). Recombinant plasmids were subsequently transformed into *Escherichia coli* BL21 (DE3) competent cells (Tiangen, China) and induced with 1 mM Isopropyl β-D-1-thiogalactopyranoside (IPTG) at 16 °C for 6 h. The his-tagged recombinant proteins were purified using an Ni^{2+}-NTA affinity chromatography column (Bio-Rad, USA), and the final protein concentrations were quantified using a bicinchoninic acid (BCA) protein assay kit (Beyotime, China).

Vaccination and parasite challenge

Eighteen beagles ($n = 6$ per group, half male and half female) were randomly assigned into three experimental groups, following the design outlined in Fig. 1. Each dog received two doses of a subcutaneous injection of the designated cocktail vaccine formulations r*Eg*ENO&r*Eg*Sev&r*Eg*Cyc and r*Eg*FABP1&r*Eg*CaM&r*Eg*Srp1 (detailed in Fig. 1), with a primary immunization at Day 0 (D0) and a booster at D14. On D21, each dog was orally challenged with 150,000 PSCs. At D49, animals were first sedated with an intramuscular injection of xylazine hydrochloride (2 mg/kg) to induce anesthesia. After confirming the absence of reflexes, euthanasia was performed by intravenous administration of sodium pentobarbital at a dose of 100 mg/kg body weight. This method was consistent with the guidelines of the American Veterinary Medical Association. The entire small intestine was excised aseptically, and the intestinal contents were systematically collected for microscopic enumeration of the total worm burden. In each dog, 50 randomly selected worms were measured for body length and maximal width. Intestinal tissue samples were fixed in 4% paraformaldehyde for subsequent histopathological assessment.

Serum IgG detection

Serum antigen-specific IgG levels were quantified using an indirect enzyme-linked immunosorbent assay (ELISA). Recombinant proteins (r*Eg*ENO, r*Eg*Sev, r*Eg*Cyc, r*Eg*FABP1, r*Eg*CaM, and r*Eg*Srp1) were coated in 96-well plates at 5 μg/mL in 0.05 M carbonate-bicarbonate buffer (pH 9.6) (100 μL/well) and incubated at 4 °C for 16 h. After three washes with PBST (0.05% Tween-20 in phosphate-buffered saline (PBS); 200 μL/well, 5 min per wash), the wells were blocked using 5% (w/v) skim milk in PBS at 37 °C for 2 h. Serum samples (diluted 1:100 in PBST) were then added and incubated at 37 °C for 1 h, followed by incubation with horseradish peroxidase (HRP)-conjugated rabbit anti-dog IgG (1:3000, Solarbio, China) at 37 °C for 1.5 h. The 3,3′,5,5′-Tetramethylbenzidine (TMB; Tiangen) substrate was added for 20 min in the dark, followed by reaction termination using 100 μL of 2 M H_2SO_4. The optical density (OD) was then measured at 450 nm.

Serum IgG longevity in dogs vaccinated with the r*Eg*ENO&r*Eg*Sev&r*Eg*Cyc vaccine was assessed using an indirect ELISA following the above protocol, with blood sera collected over 6 months.

Serum cytokine profiling

Serum levels of interleukin (IL)-2, IL-4, IL-5, IL-10, and interferon gamma (IFN-γ) were quantified using commercial ELISA kits (Solarbio, China) according to the manufacturer's instructions. Before assay execution, all kit components were equilibrated to room temperature. Standard curves were generated using recombinant cytokine calibrators provided in each kit.

Histopathological analysis

Dog small intestinal tissue samples were processed using standardized histopathological protocols. Freshly excised small intestinal segments (1 cm^3) were immediately fixed in 4% paraformaldehyde (0.1 M PBS, pH 7.4) at 4 °C for 24 h, with one solution replacement. Fixed tissues were subsequently dehydrated through a graded ethanol series, cleared in xylene, and embedded in paraffin at 56–58 °C. Serial 5 μm sections were stained with hematoxylin and eosin (H&E) and periodic acid-Schiff (PAS), followed by mounting with neutral resin. Three consecutive sections per sample were prepared.

Dog fecal microbiome profiling

Total genomic DNA was extracted from canine fecal samples using the E.Z.N.A.® DNA Kit (Omega Bio-tek, USA) following the manufacturer's instructions. The V3-V4 hypervariable regions of the 16S rRNA gene were amplified using primers 338 F (5′-ACTCCTACGGGAGGCAGCAG-3′) and 806 R (5′-GGACTACHVGGGTWTCTAAT-3′)[68]. Amplicon sequencing was performed on the Illumina NextSeq 2000 platform (Majorbio, China), and raw reads were deposited in the NCBI SRA database (Accession: PRJNA1244299).

Quality filtering and denoising of raw reads were conducted using DADA2[69] within QIIME2[70] under default parameters. Sequences were subsampled to the minimum sequencing depth (Good's coverage >99.09%) before α- and β-diversity analyses. Amplicon sequence variants (ASVs) were taxonomically classified against the SILVA 16S rRNA database (v138) using QIIME2's Naïve Bayes classifier.

Bioinformatic analyses were conducted on the Majorbio Cloud Platform (https://cloud.majorbio.com). α-Diversity indices (Chao1, Shannon) were computed using mothur[71], with intergroup differences assessed via the Wilcoxon rank-sum test. β-Diversity was evaluated via Bray–Curtis-based principal coordinate analysis (PCoA) with ANOSIM (999 permutations). Linear discriminant analysis effect size (LEfSe)[72] was used to identify differentially abundant taxa (linear discriminant analysis (LDA) > 3.5, $p < 0.05$) from phylum to genus levels. Redundancy analysis (RDA) was employed to explore cytokine-microbiome associations, while Spearman correlation networks ($p < 0.05$) were constructed to visualize key species interactions.

Statistical analysis

All parasitological parameters (total worm count, body length, and maximal width) were analyzed using SPSS 20.0 (IBM Corp., USA) and GraphPad Prism 8.0 Software (GraphPad Inc., USA). Protection efficacy was calculated as: (Mean worm burden in the control group−Mean worm burden in the vaccinated group)/Mean worm burden in the control group × 100%. The Mann–Whitney *U* test was used for statistical analysis, and differences with a *p* value less than 0.05 were considered statistically significant.

Ethics

The animal study was reviewed and approved by the Animal Care and Use Committee of Sichuan Agricultural University (SYXK2019-187). All animal procedures used in this study were carried out in accordance with the Guide for the Care and Use of Laboratory Animals (National Research Council, Bethesda, MD, USA) and recommendations of the ARRIVE guidelines (https://www.nc3rs.org.uk/arrive-guidelines). All methods were carried out in accordance with relevant guidelines and regulations.

Data availability

All data generated or analyzed during this study are included in this published article and its Supplementary Information files. The 16S rRNA gene sequence data generated in this study have been deposited in the NCBI Sequence Read Archive (accession number PRJNA1244299). The dataset is publicly accessible at: https://www.ncbi.nlm.nih.gov/bioproject/PRJNA1244299/.

Received: 2 July 2025; Accepted: 11 September 2025;
Published online: 01 October 2025

References

1. Wen, H. et al. Echinococcosis: advances in the 21st century. *Clin. Microbiol. Rev.* **32**, e00075-18 (2019).
2. Zhou, H., Wang, X., Han, S. & Xiao, N. Advances and challenges in the prevention, control and research of echinococcosis in China. *Decoding Infect. Transm.* **3**, 100041 (2025).
3. Noguera, Z. L. P., Charypkhan, D., Hartnack, S., Torgerson, P. R. & Rüegg, S. R. The dual burden of animal and human zoonoses: a systematic review. *PLoS Negl. Trop. Dis.* **16**, e0010540 (2022).

4. Widdicombe, J. et al. The economic evaluation of Cystic echinococcosis control strategies focused on zoonotic hosts: a scoping review. *PLoS Negl. Trop. Dis.* **16**, e0010568 (2022).
5. Pal, M., Alemu, H. H., Marami, L. M., Garedo, D. R. & Bodena, E. B. Cystic echincoccoosis: a comprehensive review on life cycle, epidemiology, pathogenesis, clinical spectrum, diagnosis, public health and economic implications, treatment, and control. *Int. J. Clin. Exp. Med. Res.* **6**, 131–141 (2022).
6. Rong, X., Fan, M., Zhu, H. & Zheng, Y. Dynamic modeling and optimal control of cystic echinococcosis. *Infect. Dis. Poverty* **10**, 1–13 (2021).
7. Larrieu, E., Gavidia, C. M. & Lightowlers, M. W. Control of cystic echinococcosis: background and prospects. *Zoonoses Public Health* **66**, 889–899 (2019).
8. Coffeng, L. E., Stolk, W. A. & de Vlas, S. J. Predicting the risk and speed of drug resistance emerging in soil-transmitted helminths during preventive chemotherapy. *Nat. Commun.* **15**, 1099 (2024).
9. Pourseif, M. M. et al. Current status and future prospective of vaccine development against *Echinococcus granulosus*. *Biologicals* **51**, 1–11 (2018).
10. Zhang, W. & McManus, D. P. Vaccination of dogs against *Echinococcus granulosus*: a means to control hydatid disease? *Trends Parasitol.* **24**, 419–424 (2008).
11. Craig, P. S., Giraudoux, P., Wang, Z. H. & Wang, Q. Echinococcosis transmission on the Tibetan Plateau. *Adv. Parasitol.* **104**, 165–246 (2019).
12. Craig, P., Hegglin, D., Lightowlers, M., Torgerson, P. R. & Wang, Q. Echinococcosis: control and prevention. *Adv. Parasitol.* **96**, 55–158 (2017).
13. Torgerson, P. R. Dogs, vaccines and Echinococcus. *Trends Parasitol.* **25**, 57–58 (2009).
14. Borhani, M. et al. *Echinococcus granulosus* sensu lato control measures: a specific focus on vaccines for both definitive and intermediate hosts. *Parasit. Vectors* **17**, 533 (2024).
15. Wang, N. et al. Evaluation of protective immune responses induced by DNA vaccines encoding *Echinococcus granulosus* EgM123 protein in Beagle dogs. *Front. Vet. Sci.* **11**, 1444741 (2024).
16. Zhang, W. et al. Vaccination of dogs against *Echinococcus granulosus* the cause of cystic hydatid disease in humans. *J. Infect. Dis.* **194**, 966–974 (2006).
17. Petavy, A. F. et al. An oral recombinant vaccine in dogs against *Echinococcus granulosus*, the causative agent of human hydatid disease: a pilot study. *PLoS Negl. Trop. Dis.* **2**, e125 (2008).
18. Xian, J. et al. Molecular characterization and immune protection of the 3-hydroxyacyl-CoA dehydrogenase gene in *Echinococcus granulosus*. *Parasit. Vectors* **14**, 1–11 (2021).
19. Shao, G. et al. Protective efficacy of six recombinant proteins as vaccine candidates against *Echinococcus granulosus* in dogs. *PLoS Negl. Trop. Dis.* **17**, e0011709 (2023).
20. Zimmermann, P. The immunological interplay between vaccination and the intestinal microbiota. *npj Vaccines* **8**, 24 (2023).
21. Zimmermann, P. & Curtis, N. The influence of the intestinal microbiome on vaccine responses. *Vaccine* **36**, 4433–4439 (2018).
22. Jordan, A., Carding, S. R. & Hall, L. J. The early-life gut microbiome and vaccine efficacy. *Lancet Microbe* **3**, e787–e794 (2022).
23. Lynn, D. J., Benson, S. C., Lynn, M. A. & Pulendran, B. Modulation of immune responses to vaccination by the microbiota: implications and potential mechanisms. *Nat. Rev. Immunol.* **22**, 33–46 (2022).
24. Huda, M. N. et al. Stool microbiota and vaccine responses of infants. *Pediatrics* **134**, e362–e372 (2014).
25. Mullié, C. et al. Increased poliovirus-specific intestinal antibody response coincides with promotion of Bifidobacterium longum-infantis and Bifidobacterium breve in infants: a randomized, double-blind, placebo-controlled trial. *Pediatr. Res.* **56**, 791–795 (2004).
26. Harris, V. et al. Rotavirus vaccine response correlates with the infant gut microbiota composition in Pakistan. *Gut Microbes* **9**, 93–101 (2018).
27. Zhao, T. et al. Influence of gut microbiota on mucosal IgA antibody response to the polio vaccine. *npj Vaccines* **5**, 47 (2020).
28. Harris, V. C. et al. Significant correlation between the infant gut microbiome and rotavirus vaccine response in rural Ghana. *J. Infect. Dis.* **215**, 34–41 (2017).
29. Walusimbi, B. et al. The effects of helminth infections on the human gut microbiome: a systematic review and meta-analysis. *Front. Microbiomes* **2**, 1174034 (2023).
30. Sieng, S., Chen, P., Wang, N., Xu, J.-Y. & Han, Q. Toxocara canis-induced changes in host intestinal microbial communities. *Parasit. Vectors* **16**, 462 (2023).
31. Paz, E. A. et al. Bacterial communities in the gastrointestinal tract segments of helminth-resistant and helminth-susceptible sheep. *Anim. Microbiome* **4**, 23 (2022).
32. Su, C. et al. Helminth-induced alterations of the gut microbiota exacerbate bacterial colitis. *Mucosal Immunol.* **11**, 144–157 (2018).
33. Hua, R. Q. et al. Genetic diversity of *Echinococcus granulosus* sensu lato in China: epidemiological studies and systematic review. *Transbound. Emerg. Dis.* **69**, e1382–e1392 (2022).
34. Jorge, S. & Dellagostin, O. A. The development of veterinary vaccines: a review of traditional methods and modern biotechnology approaches. *Biotechnol. Res Innov.* **1**, 6–13 (2017).
35. Torgerson, P. Canid immunity to Echinococcus spp.: impact on transmission. *Parasite Immunol.* **28**, 295–303 (2006).
36. Wang, Y. et al. Impairment of dendritic cell function and induction of CD4+ CD25+ Foxp3+ T cells by excretory-secretory products: a potential mechanism of immune evasion adopted by *Echinococcus granulosus*. *BMC Immunol.* **16**, 1–10 (2015).
37. Cao, S. et al. Arginase promotes immune evasion of *Echinococcus granulosus* in mice. *Parasit. Vectors* **13**, 1–12 (2020).
38. Siracusano, A. et al. Immunomodulatory mechanisms during *Echinococcus granulosus* infection. *Exp. Parasitol.* **119**, 483–489 (2008).
39. Ammar, A., Elleboudy, N. & Mohammed, S. The contribution of in silico studies in parasitology: a multifaceted approach. *Parasitol. U. J.* **16**, 1–11 (2023).
40. Zheng, H. et al. The genome of the hydatid tapeworm *Echinococcus granulosus*. *Nat. Genet.* **45**, 1168–1175 (2013).
41. Li, Z. J. & Wei, Z. Analysis of protoscoleces-specific antigens from *Echinococcus granulosus* with proteomics combined with Western blot. *Biomed. Environ. Sci.* **25**, 718–723 (2012).
42. Miles, S. et al. Combining proteomics and bioinformatics to explore novel tegumental antigens as vaccine candidates against *Echinococcus granulosus* infection. *J. Cell Biochem.* **120**, 15320–15336 (2019).
43. Pourseif, M. M., Yousefpour, M., Aminianfar, M., Moghaddam, G. & Nematollahi, A. A multi-method and structure-based in silico vaccine designing against *Echinococcus granulosus* through investigating enolase protein. *Bioimpacts* **9**, 131 (2019).
44. Miles, S., Velasco-de-Andrés, M., Lozano, F. & Mourglia-Ettlin, G. Interactome analysis of CD5 and CD6 ectodomains with tegumental antigens from the helminth parasite *Echinococcus granulosus* sensu lato. *Int. J. Biol. Macromol.* **164**, 3718–3728 (2020).
45. Zhang, X. et al. EgSeverin and Eg14-3-3zeta from *Echinococcus granulosus* are potential antigens for serological diagnosis of echinococcosis in dogs and sheep. *Micro. Pathog.* **179**, 106110 (2023).
46. Khazaei, S. & Moghadamizad, Z. *Echinococcus granulosus* cyclophilin: Immunoinformatics analysis to provide insights into the biochemical properties and immunogenic epitopes. *Inf. Med. Unlocked* **30**, 100925 (2022).

47. Chabalgoity, J. A. et al. Expression and immunogenicity of an *Echinococcus granulosus* fatty acid-binding protein in live attenuated Salmonella vaccine strains. *Infect. Immun.* **65**, 2402–2412 (1997).
48. Mousavi, S. M. et al. Calmodulin-specific small interfering RNA induces consistent expression suppression and morphological changes in *Echinococcus granulosus*. *Sci. Rep.* **9**, 3894 (2019).
49. Wang, N. et al. Molecular and biochemical characterization of calmodulin from *Echinococcus granulosus*. *Parasit. Vectors* **10**, 1–9 (2017).
50. Guo, G., Tian, M. X., Jiao, H. J., Li, J. & Zhang, W. B. Comparison and analysis of structure and function of serine protease inhibitors from two strains of Echinococcus. *Chin. J. Biol.* **34**, 928–935 (2021).
51. Li, X. et al. *Echinococcus multilocularis* serpin regulates macrophage polarization and reduces gut dysbiosis in colitis. *Infect. Immun.* **92**, e00232-24 (2024).
52. Rivero, F. D. et al. Disruption of antigenic variation is crucial for effective parasite vaccine. *Nat. Med.* **16**, 551–557 (2010).
53. Lightowlers, M. et al. Vaccination against cestode parasites: anti-helminth vaccines that work and why. *Vet. Parasitol.* **115**, 83–123 (2003).
54. Manjunathachar, H. V. et al. Cocktail vaccine for the management of Hyalomma anatolicum and Rhipicephalus microplus. *Front. Immunol.* **15**, 1471317 (2024).
55. Woolsey, I. D. & Miller, A. L. *Echinococcus granulosus* sensu lato and *Echinococcus multilocularis*: a review. *Res. Vet. Sci.* **135**, 517–522 (2021).
56. Borey, M. et al. Links between fecal microbiota and the response to vaccination against influenza A virus in pigs. *npj Vaccines* **6**, 92 (2021).
57. Ciabattini, A., Olivieri, R., Lazzeri, E. & Medaglini, D. Role of the microbiota in the modulation of vaccine immune responses. *Front. Microbiol.* **10**, 1305 (2019).
58. Sanmarco, L. M. et al. Lactate limits CNS autoimmunity by stabilizing HIF-1α in dendritic cells. *Nature* **620**, 881–889 (2023).
59. Beyhan, Y. E. & Yıldız, M. R. Microbiota and parasite relationship. *Diagn. Microbiol. Infect. Dis.* **106**, 115954 (2023).
60. Yang, C. A. et al. Impact of Enterobius vermicularis infection and mebendazole treatment on intestinal microbiota and host immune response. *PLoS Negl. Trop. Dis.* **11**, e0005963 (2017).
61. Wang, Y. et al. Proteomic analysis of the excretory/secretory products and antigenic proteins of *Echinococcus granulosus* adult worms from infected dogs. *BMC Vet. Res.* **11**, 1–7 (2015).
62. Cortés, A., Muñoz-Antoli, C., Esteban, J. G. & Toledo, R. Th2 and Th1 responses: clear and hidden sides of immunity against intestinal helminths. *Trends Parasitol.* **33**, 678–693 (2017).
63. McFarlane, A. J. et al. Enteric helminth-induced type I interferon signaling protects against pulmonary virus infection through interaction with the microbiota. *J. Allergy Clin. Immunol.* **140**, 1068–1078 (2017).
64. Zhan, J. et al. Molecular and functional characterization of inhibitor of apoptosis proteins (IAP, BIRP) in *Echinococcus granulosus*. *Front. Microbiol* **11**, 729 (2020).
65. Perkins, D. N., Pappin, D. J., Creasy, D. M. & Cottrell, J. S. Probability-based protein identification by searching sequence databases using mass spectrometry data. *Electrophoresis* **20**, 3551–3567 (1999).
66. Virginio, V. G. et al. Excretory/secretory products from in vitro-cultured *Echinococcus granulosus* protoscoleces. *Mol. Biochem. Parasitol.* **183**, 15–22 (2012).
67. Nicolao, M. C., Rodriguez Rodrigues, C. & Cumino, A. C. Extracellular vesicles from *Echinococcus granulosus* larval stage: isolation, characterization and uptake by dendritic cells. *PLoS Negl. Trop. Dis.* **13**, e0007032 (2019).
68. Liu, C. et al. Denitrifying sulfide removal process on high-salinity wastewaters in the presence of Halomonas sp. *Appl. Microbiol. Biotechnol.* **100**, 1421–1426 (2016).
69. Edgar, R. C. UPARSE: highly accurate OTU sequences from microbial amplicon reads. *Nat. Methods* **10**, 996–998 (2013).
70. Barberán, A., Bates, S. T., Casamayor, E. O. & Fierer, N. Using network analysis to explore co-occurrence patterns in soil microbial communities. *ISME J.* **6**, 343–351 (2012).
71. Schloss, P. D. et al. Introducing mothur: open-source, platform-independent, community-supported software for describing and comparing microbial communities. *Appl. Environ. Microbiol.* **75**, 7537–7541 (2009).
72. Segata, N. et al. Metagenomic biomarker discovery and explanation. *Genome Biol.* **12**, 1–18 (2011).

Acknowledgements

The authors gratefully acknowledge all the participants involved in the dog vaccine development for their invaluable contributions. We also extend our sincere appreciation to the staff of the Beagles Breeding Center for their dedicated assistance with animal management. This work was supported by a grant from the Key Technology Research and Development Program of Sichuan Province in China (grant number 2022YFN0013).

Author contributions

G.Y. and A.Y. conceived and designed the study, contributed to funding acquisition and data verification. G.S., R.H. and X.Z. were responsible for conducting experiments, performing data analysis and drafting the manuscript. Y.C. and Z.L. contributed to project administration and data collection. All authors read and approved the final version of the manuscript.

Competing interests

The authors declare no competing interests.

Additional information

Supplementary information The online version contains supplementary material available at https://doi.org/10.1038/s41541-025-01275-x.

Correspondence and requests for materials should be addressed to Guangyou Yang.